



# Incremental forming of Titanium T40 sheet: experimental and numerical investigations

A. Abdelkefi, D. Guines, L. Leotoing, S. Thuillier

## ► To cite this version:

A. Abdelkefi, D. Guines, L. Leotoing, S. Thuillier. Incremental forming of Titanium T40 sheet: experimental and numerical investigations. 24ème Congrès Français de Mécanique, Aug 2019, Brest, France. hal-02328578

**HAL Id: hal-02328578**

**<https://hal.archives-ouvertes.fr/hal-02328578>**

Submitted on 23 Oct 2019

**HAL** is a multi-disciplinary open access archive for the deposit and dissemination of scientific research documents, whether they are published or not. The documents may come from teaching and research institutions in France or abroad, or from public or private research centers.

L'archive ouverte pluridisciplinaire **HAL**, est destinée au dépôt et à la diffusion de documents scientifiques de niveau recherche, publiés ou non, émanant des établissements d'enseignement et de recherche français ou étrangers, des laboratoires publics ou privés.

# Incremental forming of Titanium T40 sheet: experimental and numerical investigations

A. Abdelkefi<sup>a</sup>, D. Guines<sup>a</sup>, L. Léotoing<sup>a</sup>, S. Thuillier<sup>b</sup>

a. Univ. Rennes, INSA Rennes, LGCGM - EA 3913, F-35000 Rennes, France,  
abir.abdelkefi@insa-rennes.fr, dominique.guines@insa-rennes.fr, lionel.leotoing@insa-  
rennes.fr

b. Univ. Bretagne Sud, UMR CNRS 6027, IRDL, F-56100 Lorient, France,  
sandrine.thuillier@univ-ubs.fr

## Résumé :

*Le procédé de formage incrémental mis en œuvre avec un poinçon unique et de forme simple (SPIF) présente un fort potentiel pour la fabrication en petites séries de produits personnalisés et de formes complexes. Au cours du procédé SPIF, la tôle est bridée et un outil hémisphérique la déforme localement, de manière itérative, en suivant une trajectoire bien spécifique. L'utilisation de robots industriels pour mettre en œuvre ce procédé a pour objectif d'améliorer sa flexibilité (augmentation du volume de travail et complexité accrue des pièces formées) et de diminuer son coût de revient. Pour ces systèmes mécaniques, dont la rigidité structurelle est faible, la prédiction des efforts de formage associée au modèle élastique du robot est nécessaire pour compenser les erreurs de trajectoire de l'outil et pour garantir la qualité géométrique de la pièce finale. Les efforts de formage peuvent être prédits à partir d'une simulation par éléments finis du procédé et utilisés ensuite comme données d'entrée du modèle élastique du robot. Cependant, la précision des efforts calculés dépend fortement du modèle de comportement du matériau constitutif du flan introduit dans la simulation du procédé SPIF. Dans ce contexte, l'objectif de cette étude est d'évaluer l'aptitude d'un modèle elasto-plastique simple, identifié à partir d'essais de traction conventionnels réalisés sur un alliage de titane T40, à prédire les efforts de formage mis en jeu lors du formage d'un cône tronqué. L'évaluation du modèle est réalisée en comparant les résultats (efforts et géométrie) numériques et expérimentaux.*

## Abstract:

*Single point incremental forming process (SPIF) has a great potential to manufacture small series of customized products. During SPIF process, the sheet metal is clamped and locally deformed, in an iterative way, by a hemispherical tool that follows a specified trajectory. The use of industrial robots to implement this process aims to improve its flexibility (increased volumes of work and complexity of the formed parts) and to reduce its cost. For these mechanical systems, for which the structural rigidity is low, the prediction of forming forces associated to an elastic modeling of the robot is necessary to compensate tool path errors due to the robot compliance and to ensure the geometrical quality of the final part. The forming forces can be predicted from a finite element simulation of the process and used then as input data to the elastic modeling of the robot. However, the accuracy of the calculated loads depends strongly on the constitutive material behavior of the blank introduced in the*

*simulation of the SPIF process. In this context, the aim of this study is to evaluate the ability of a simple elasto-plastic model, identified from conventional tensile tests carried out on a T40 titanium alloy, to predict the forming loads used to manufacture a truncated cone. The evaluation of the model is performed by comparing numerical predictions with the experimental results (efforts and geometry).*

**Keywords: Single point incremental forming process; mechanical model; experimental test; numerical simulation; forming load.**

## 1 Introduction

During the last decades, several authors pay attention to the incremental forming process (SPIF) due to its ability to manufacture complex shapes using simple tool. Usually, the forming operation is performed by classical three-axis CNC machines with high stiffness. A solution to improve the production flexibility and to reduce manufacturing costs is to use robots connected in serial or parallel. Nevertheless, they present some drawbacks such as high compliance and low positioning precision under high loading [1]. To improve the accuracy of the robotized process, an approach coupling the Finite Element Analysis (FEA) of the process with the elastic modeling of robot structure is proposed [1]. In order to evaluate tool path deviation, FEA is used to predict the forming loads which are used as input in the elastic model of the robot. To the author's knowledge, only a few studies have investigated the influent parameters on the forces predicted by FEA. Henrard et al. [2] and Flores et al. [3] have compared the influence of different plastic behaviors (yield criterion, hardening law, hardening type) on the force prediction for AA3003-O. Results show that forming forces depend more on the hardening law than on the yield locus and the use of kinematic hardening leads to a noticeable drop (up to 20%) of the estimated forces. However, Ben Said et al. [4] have also shown that the prediction of tool forces depends both on the hardening law and yield criterion. Moreover, the use of isotropic hardening leads to a high value of the predicted forces in comparison with the ones obtained from a mixed hardening model. The same conclusion is drawn by Benedetti et al. [5], they found that the use of mixed hardening seems to be more suitable to predict the forming loads. From these previous studies, it should be highlighted that the selection of a suitable material model to predict accurate forming forces is still a challenging task. These difficulties mainly lie in high plastic strain levels (larger than 100%) and complex strain paths observed in this process [3]. For these reasons, material parameters should be carefully identified.

Among the typical materials used to manufacture complex shapes for SPIF process, titanium stands out due to its high strength to weight ratio, inertness, and bio-compatibility [6]. In terms of experimental characterization of titanium alloy to identify material parameters for the numerical simulation of SPIF process, detailed studies remain few in literature. Saidi et al. [7] and Sakhtemanian et al. [8] have used tensile tests to identify T40 alloy parameters to make truncated cone and pyramid, respectively. Lino et al. [9] have used tensile tests at several orientations and bulge test, for the same material, to manufacture a medical implant.

In this paper, an experimental investigation covering both the mechanical characterization of T40 alloy and the manufacturing of a truncated cone are carried out in section 2. A numerical approach of the SPIF process using a simple elasto-plastic model is proposed in section 3. In section 4, the evaluation of the model is performed by comparing numerical predictions with the experimental results (efforts and geometry).

## 2 Experiments

### 2.1 Mechanical behavior of T40 alloy

The sheet material considered in this work is the T40 titanium alloy often used in aeronautical and biomedical industries due to its formability and its corrosion resistance. This sheet material is generally suitable for SPIF process and forming applications [7-9]. T40 sheets are received as cold-rolled blank with a thickness of 0.5 mm. The chemical composition of the T40 alloy is given in Table 1. The mechanical behavior is investigated by means of uniaxial tensile tests performed at several orientations to the rolling direction, simple shear and bulge tests. However, in a first step, only isotropic hardening associated with von Mises yield criterion is considered and only the mechanical behavior in tension in the rolling direction (Fig. 1) is used. Mechanical properties are then calculated, leading as average values over three tests to  $R_{p0.2\%} = 215$  MPa and  $R_m = 328$  MPa.

Table 1: Chemical composition (in wt %) of the T40 alloy.

Fe	C	N	H	O	Ti
0.3	0.08	0.03	0.015	0.25	bal.

The elastic behavior of the material is defined by the Young modulus  $E = 110$  GPa and the Poisson ratio  $\nu=0.3$ . The plastic behavior is modeled by the Swift law  $\bar{\sigma} = K * (\varepsilon_0 + \bar{\varepsilon}_p)^n$  where  $\bar{\sigma}$  is the equivalent stress,  $\varepsilon_0 = (\sigma_0/K)^{1/n}$  and  $\bar{\varepsilon}_p$  is the equivalent plastic strain,  $K = 630$  MPa,  $\sigma_0 = 205$  MPa and  $n = 0.3$ . Swift parameters are identified from the tensile test results.

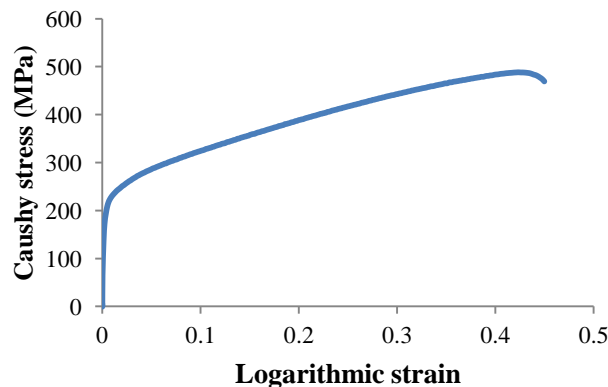


Figure 1. Stress strain curve of T40 in tension in the rolling direction. Necking occurs at  $\varepsilon = 0.3$  but the Cauchy stress is still calculated above this point.

### 2.2 Experimental SPIF process

For the designed part, a T40 square sheet of  $270 \times 270 \times 0.5$  mm<sup>3</sup> is used to form a frustum cone of 45° wall angle (Fig. 2(a)). The depth of the truncated cone is 30 mm. The forming tool is a hemispherical punch with a 15 mm diameter. The feed rate value of the tool is 360 mm/min and the tool rotation is locked. The SPIF operation is carried out on a three axis CNC milling machine (Famup MCX600). The tool path consists of successive circular contours at constant Z. The incremental step size value  $\Delta Z$  is 1mm per loop. The forming forces applied by the tool are measured by a six-axes force/torque sensor ATI Omega190. The clamping system (Fig. 2(b)) is composed of a blank holder screwed on a

rigid frame. The contact between tool and sheet is lubricated to minimize the value of the friction coefficient. The duration of the forming operation is about 30 min.

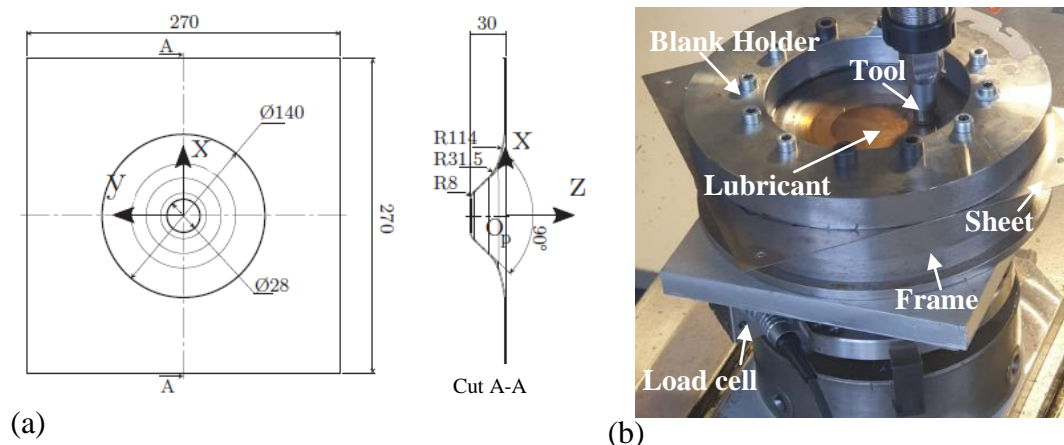


Figure 2. Experimental setup (a) shape of 45° wall angle truncated cone (dimensions in millimeters), (b) incremental forming device

Figure 3 presents the forming force  $F_Z$  measured in the axial direction of the tool. At the end of each circular path at constant  $Z$ , the imposed tool path leads to the loss of contact between the tool and the sheet metal, which results in a return of the force  $F_Z$  to zero. At each new  $Z$ -increment, the tool-to-sheet contact restoration generates a peak force, especially for the deepest passes. As shown on the zoom, figure 3, for a circular path at  $Z = 26 \text{ mm}$ , the force  $F_Z$  then stabilizes quickly from the beginning of the considered path and is relatively constant over one revolution. The same tendencies have been observed in previous works [1-5]. The axial load  $F_Z$  increases gradually during successive increments of the tool  $Z$ -positions, reaches then a maximum value of 910 N and remains stable around this value until the end of forming. At the end of the forming process, the clamped part is measured by a 3D laser measurement system.

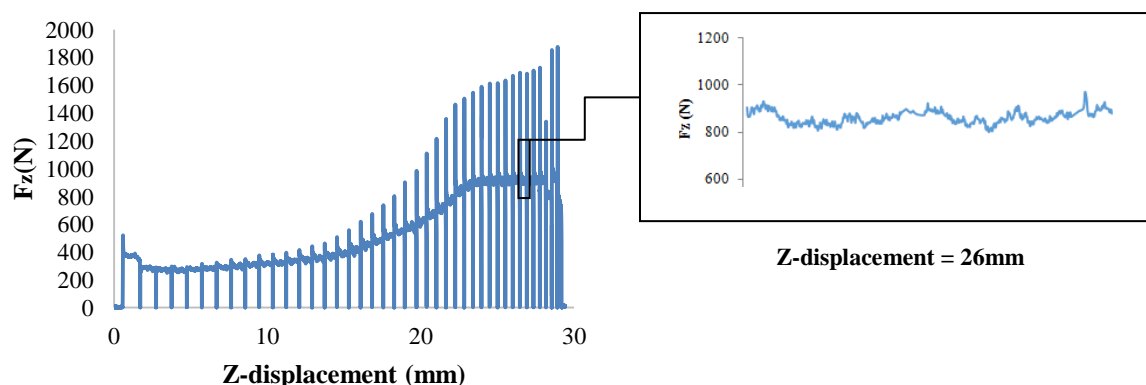


Figure 3. Force measurement along the tool axis. The zoom on the right-hand side corresponds to the load evolution during a circular path at a constant  $Z$ -position.

### 3 Finite element analysis (FEA)

In this section, the full process simulation is carried out using Abaqus/implicit© software. To reduce computation time, only one fourth of the blank is considered, though the problem is not symmetric.

However, such a simplified model was compared to the full one, showing very comparable results. Four node shell elements with reduced integration (S4R) are employed to model the sheet. The x-axis corresponds to the rolling direction of the sheet. The X and Y axes are also the symmetry axes of the reduced model. The hemispherical punch is modeled as a rigid body. An embedding condition is applied along the outer circular edge (corresponding to the 140 mm diameter in Fig. 4). Frictionless contact is considered between the tool and the sheet. The sheet is modeled as an elastic-plastic material associated with von Mises yield criterion (section 2.1).

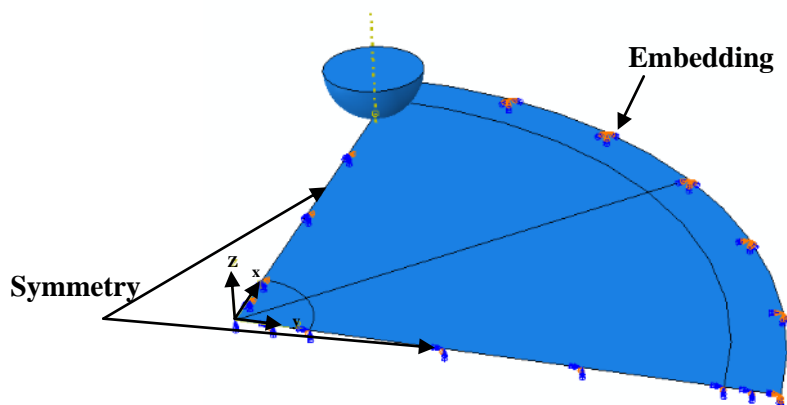
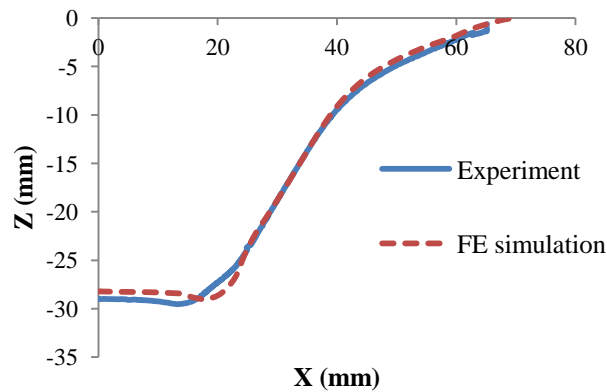


Figure 4. FE model with boundary conditions

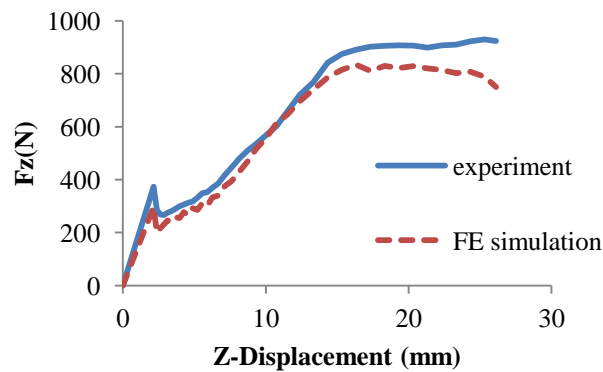
## 4 Discussion

A comparative study of the experimental and numerical results of the final part geometry, before the unclamping stage, is presented in Fig. 5a. For the simulation, the part profile is taken from the median plane of the model shown in Fig. 4, which corresponds to a 45° cutting plane of the XZ plane. For the formed part, the measured profile corresponds to the bottom side of the sheet metal (on the opposite side to the tool with respect to the sheet). As shown in Fig. 5(a), FE simulation predicts well the wall region and underestimates the cone bottom. As explained in previous studies [10-11], if the constitutive model is not a key factor to predict accurately the final experimental geometry, the use of a reduced or full numerical model seems to be more influent [3]. Differences observed in Fig. 5(a) can be explained by the modeling adopted here, i.e. one fourth of the blank is modeled and symmetry conditions are applied on X and Y axes.

Figure 5b presents a comparison between experimental and simulated forces in Z-direction. The average of the vertical force over one cycle (at Z-constant) is calculated and used in the comparison between experiments and simulation. As shown in Fig. 5(b), the force reaches a steady maximum value after a Z-displacement of about 15 mm. The FE model noticeably underestimates the steady value of the forming load, with a relative gap of 11%. This mismatch can be explained by several reasons: i) shell element model seems not to be suitable to represent the transversal shear deformation which is considered not negligible by some authors [5]; ii) the choice of isotropic hardening and isotropic yield criterion does not represent accurately the material behavior, iii) the use of an embedding condition may not be suitable to model the real boundary conditions applied to the blank during the SPIF process.



(a)



(b)

Figure 5. Comparison between experiments and FE predictions (a) geometry of the final shape (b) vertical load as a function of the tool displacement

## 5 Conclusion

In the present study, the SPIF process is investigated through experimental and numerical approaches. Mechanical characterization is led by means of uniaxial tensile tests to identify the material parameters of the T40 titanium alloy. A FE simulation of a SPIF operation of a truncated cone is performed using a simple elasto-plastic model. Impact of the proposed model on the final geometry and the forming load is investigated. It is concluded that the final geometry is rather well predicted but the final forming load is underestimated by 11%. In the future, in order to improve the prediction of the forming loads, additional numerical analysis of the SPIF process will be performed to check influent parameters on the predicted forces such as mechanical models, boundary conditions and element types.

## References

- [1] J. Belchior, L. Leotoing, D. Guines, E. Courteille, and P. Maurine, A process/ Machine coupling approach: Application to robotized incremental sheet forming, *Journal of Materials Processing Technology*, 214 (2014), 1605-1616.

- [2] C. Henrard, C. Bouffieux, P. Eyckens, H. Sol, J.R. Duflou, P. Van Houtte, A. Van Bael, L. Duchêne, and A.M. Habraken, Forming forces in single point incremental forming: prediction by finite element simulations, validation and sensitivity, *Computational mechanics*, 47 (2011), 573-590.
- [3] P. Flores, L. Duchene, C. Bouffieux, T. Lelotte, C. Henrard, N. Pernin, A. Van Bael, S. He, J. Duflou, and A.M. Habraken, Model identification and FE simulations: effect of different yield loci and hardening laws in sheet forming, *International journal of plasticity*, 23 (2007), 420-449.
- [4] L.B. Said, J. Mars, M. Wali, F. Dammak, Numerical prediction of the ductile damage in single point incremental forming process, *International Journal of Mechanical Sciences*, 131 (2017), 546-558.
- [5] M. Benedetti, V. Fontanari, B. Monelli, M. Tassan, Single-point incremental forming of sheet metals: Experimental study and numerical simulation, *Proceedings of the Institution of Mechanical Engineers, Part B: Journal of Engineering Manufacture*, 231 (2017), 301-312.
- [6] B.P. Bannon, E.E. Mild, Titanium Alloys for Biomaterial Application: An Overview, *Titanium Alloys in Surgical Implants: A Symposium ASTM STP*, 796 (1983) 7-16.
- [7] B. Saidi, G. Laurence, M. Boulila, A. Cherouat, and R. Nasri, Etude expérimentale et numérique des efforts lors du formage incrémental de tôles en titane, *JET 2016, Hammamet, Tunisie*.
- [8] M.R. Sakhtemanian, M. Honarpisheh, S. Amini, Numerical and experimental study on the layer arrangement in the incremental forming process of explosive-welded low-carbon steel/CP-titanium bimetal sheet, *International Journal of Advanced Manufacturing Technology*, 95 (2018), 3781-3796.
- [9] J. Lino, R. Aarajuo, P. Teixeira, M.B. Silva, A. Reis, and P. Martins, Single point incremental forming of a medical implant, *Key Engineering Materials, Trans Tech Publications*, 554 (2013), 1388-1393.
- [10] C. Henrard, A.M. Habraken, A. Szekeres, J.R. Duflou, S. He, A. Van Bael, P. Van Houtte, Comparison of FEM simulations for the incremental forming process, *Advanced Materials Research*, 6-8 (2005), 533-542.
- [11] S. He, A. Van Bael, P. Van Houtte, A. Szekeres, J.R. Duflou, C. Henrard, A.M. Habraken, Finite element modeling of incremental forming of aluminum sheets, *Advanced Materials Research*, 6-8 (2005), 525-532.